Research on Heartbeat Detection Method of Ballistocardiogram based on Bidirectional long short-term memory network

GENG PANG[1,2], DUYAN GENG[1,2]

[1]State Key Laboratory of Reliability and Intelligence of Electrical Equipment, Hebei University of Technology, Tianjin 300130, CHINA
[2]School of Electrical Engineering, Hebei University of Technology,Tianjin 300130, China
3School of Health Sciences&Biomedical Engineering, Hebei University of Technology, Tianjin 300130, CHINA

Abstract: In order to improve the accuracy and generalization ability of extracting successive heartbeat cycle based on ballistocardiogram (BCG), this paper proposed a general method for detecting J peak of BCG signals by using bidirectional long short-term memory network. First, the clustering method is used to establish the sequence feature set of BCG signals in different sleeping positions, and the data set used contains a variety of different forms of BCG signals. Then, according to the Bidirectional LSTM (BiLSTM) many-to-many recognition model, the number of J peaks in the output sequence is counted to achieve real-time heartbeat detection. The results showed that the deviation rate of BCG heart rate detection was 0.27%, and there was no significant difference between BCG and ECG in the detection of heartbeat interval. Compared with other methods, this method has higher robustness and accuracy in detection effect, which provides a new idea for realizing high-precision unconstrained heartbeat detection.

Keywords: Ballistocardiogram, Bidirectional LSTM, Heart rate detection, Sequence feature learning

Received: May 28, 2021. Revised: March 20, 2022. Accepted: April 23, 2022. Published: June 28, 2022.

1. Introduction

Cardiovascular disease is the main cause of death [1]. The acquisition of heartbeat information through wearable or non-contact devices is of great significance in sleep quality assessment, cardiovascular health monitoring and mental state recognition. In view of the inevitable contact interference and relatively specialized operation process of electrocardiography (ECG) acquisition, the non-contact ballistocardiography (BCG) technology suitable for home environment has attracted much attention. Heart rate estimation based on ballistocardiogram has the advantages of non-invasive, simple operation and low cost, and the resulting problem of heartbeat detection accuracy has become a bottleneck restricting its application.

BCG signals are mechanical signals produced by heart beats, which reflects the mechanical characteristics of the heart [2-4], and can show changes in the body's external pressure or body surface displacement caused by the heart's pumping activity. A typical BCG signal is shown in the Fig. 1, which mainly contains 7 peaks such as H, I, J, K, L, M and N peaks. Usually, H, I, J, K and L peaks are regarded as a BCG signal complex to represent a heartbeat [5]. The J peak in BCG signal corresponds to the R peak in electrocardiogram (ECG) [6], which represents the maximum amplitude point of a cardiac cycle in the signal. Therefore, accurate J peak positioning is the key to achieve BCG signals heartbeat detection.

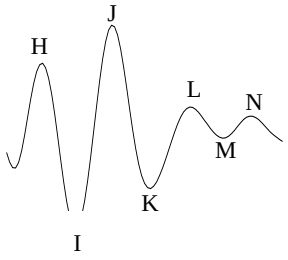

Figure 1. Standard ballistocardiograms heartbeat pattern

In recent years, the utilization of BCG signals for heart rate statistics and prediction has been studied by researchers. These algorithms are mainly based on threshold detection [7-8], template matching [9-10] or machine learning theory. The threshold method generally identifies J peaks by conventional peak detection methods, and finding local maxima within windows as potential heartbeat locations. This method is most susceptible to interference, including individual differences, acquisition mode differences, and BCG signal oscillations, among others. The template matching method is to construct a template database by collecting I-J-K composite wave of BCG, achieve template matching by means of a locally moving window function, and detect heartbeats according to correlation coefficients. This method can obtain better results when template matching is consistent. However, the adaptability of the heartbeat template will be reduced due to the influence of individual differences, or the position movement of subjects and the change of limb state. Machine learning method [11-12] uses unsupervised learning clustering or Gaussian mixture model clustering algorithm to distinguish J peaks and other peaks to

calculate the BCG signals peak group characteristics, and then calculate the heartbeat interval. Clustering algorithm has strong dependencies on BCG signals with standard morphology and single mode, and the accuracy of extracting J peaks tends to be somewhat lower than supervised learning. However, due to less training steps, simple process and fast output results of clustering algorithm, clustering algorithm can efficiently label BCG signal peak classes, thereby providing a role for supervised learning.

In the actual acquisition process, BCG signals exhibit different morphologies due to noise interference, individual variations, acquisition modalities and acquisition equipment. The morphological changes are manifested in the relative changes of the amplitude and distance of each peak, and the peak group model is no longer obvious. In summary, the instability of BCG morphology needs to be taken into account when using BCG signals to extract heart rate. Detection based on the intrinsic temporal features of BCG complex is the key to solving such problems. Long Short-Term Memory network (LSTM) excels at extracting features from sequences and can make predictions for each data in sequences. Since heart rate information is rich in temporal characterization, LSTM network have been widely used in heart rate information research [13-15]. There have been studies applying LSTM on BCG signals to calculate heart rate [16], but this method simply calculates the approximate heart rate of a certain segment of the signal and cannot accurately localize the heartbeat cycle.

Therefore, this paper proposes a heartbeat detection method based on BiLSTM for J peak localization of BCG signals. By dividing BCG sequence segments and extracting peak feature parameters as input, the BiLSTM advanced semantic recognition model is used to classify BCG peaks in the test set. The heart rate is calculated according to the classification results of the J peaks, and the accuracy is compared with the labels in the data set to verify the effectiveness of the method in this paper.

2. Methods

2.1 Dataset

Since there is no uniform standard for the sensors, measurement positions, and methods used to collect BCG signals, there is no recognized standard BCG database. The BCG dataset used in this study need to be collected and labeled independently. A total of 28 volunteers were recruited in the experiment, ranging in age from 18 to 50 years old, with 16 males and 12 females. The 28 subjects were defined as P1~P28. The BCG signals acquisition equipment uses DEEBCG ballistocardiography (DeE Software Co., Ltd. Zhejiang, China). As shown in Fig. 2a, after the signal is collected by the device, it is denoised and uploaded to the cloud, and the data is obtained at the client. The data acquisition process is shown in Figure 2b. The subject lies flat on the bed, and the sensor is placed under the pillow. The data is collected in the four sleeping positions of supine, prone, left and right for 10min respectively.

Figure 2. (a) Acquisition equipment (b) Signal acquisition process

In order to obtain the ECG signals as the reference standard synchronously, each subject used the three-lead ECG acquisition system designed by the research group. The R peaks are detected using the Pan-Tumpkins algorithm [17], and the RR interval are calculated as the reference ("ground truth") data.

Experimental data need to be labeled for each peak and entered as a sequence fragment. Clustering algorithm can divide unlabeled data into several disjoint subsets according to certain rules [18]. The similarity within the same subset is as large as possible, the similarity between subsets is as small as possible. According to the characteristics of BCG complex showing regularity and periodicity in a continuous period of time, K-means clustering algorithm is used to distinguish various types of BCG peaks when labeling each BCG J peaks. The algorithm steps are as follows:

(1) Search all peaks and troughs of the signal in the interval and the corresponding index positions,

(2) Use all the peak and trough data for parameter calculation, as shown in Fig. 3, 4 parameters are calculated for each peak, which are the amplitude Pa(n) of the peak P(n), the amplitude Ta(n) of the trough T(n) adjacent to the peak P(n), the distance Pd(n) between the peak P(n) and the trough T(n), and the distance Td(n) between the trough T(n) and the next peak P(n+1). Take the parameters of 5 consecutive peaks as the eigenvector of the first peak to construct a feature set, each eigenvector has a total of 20 parameters, the eigenvector $\boldsymbol{f_n}$ is:

$$f_n = \begin{pmatrix} Pa(n), Ta(n), Pd(n), Td(n), \ldots, \\ Pa(n+4), Ta(n+4), Pd(n+4), Td(n+4) \end{pmatrix} \quad (1)$$

(3) The K-means algorithm is used to cluster the feature set. The number of clusters is 5 and the distance is Euclidean distance. The best arrangement is selected in the five initializations, and the peak group index after clustering is confirmed.

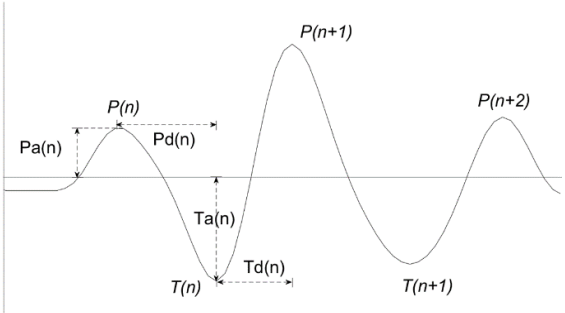

Figure 3. Characteristic parameters of peaks and troughs

After classifying each peak, proceed to the next step of processing and labeling, the steps are as follows:

(1) The J-wave results were manually checked against the synchronously acquired ECG signals. The criteria are as follows: whether the J peak is between two adjacent R peaks; whether the number of J peaks is consistent with the number of R peaks. After verification, unrecognized or incorrectly recognized J peaks are corrected according to the peak index, so as to ensure the quality of the data set.

(2) According to the J peak index, locate the H peak and L peak index respectively. In each BCG sequence, J peak is labeled as 1, H peak is labeled as 2, L peak is labeled as 3, and the rest peaks are labeled as 0. An example of the labeling result is shown in Figure 4.

(3) After labeling the peaks, each BCG signal is segmented according to every 100 peaks as a sequence, and the remaining fragments with less than 100 peaks are filled with 0. The dataset finally contains 1190 heartbeat sequences, with a total of 19375 heartbeats.

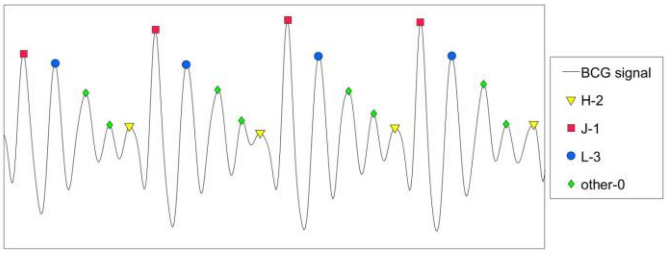

Figure 4. Peaks marking results

2.2 Model Training

BiLSTM consists of forward LSTM and backward LSTM. LSTM is a special recurrent neural network (RNN), and its cell structure is shown in Fig. 4. Each cell unit contains three gating units: input gate, forget gate and output gate. The output is determined by the current state of the cell and the gate authority, which can effectively solve the vanishing gradient problem [19]. When each cell unit works, it first passes through the forget gate to determine how much information to retain from the original cell's memory. The calculation formula of forget door is:

$$\Gamma_f = \sigma\left(w_f\left[h^{(t-1)}, x^{(t)}\right] + b_f\right) \quad (2)$$

where, σ is the sigmoid activation function, w_f is the forget gate weight matrix, $h^{(t-1)}$ is the hidden layer state at time (t-1), $x^{(t)}$ is the input at time t, and b_f is the forget gate intercept.

Next, the proportion of new information stored in the new cell state is determined through the input gate. The input gate expression and cell state correction value expression are:

$$\Gamma_i = \sigma\left(w_i\left[h^{(t-1)}, x^{(t)}\right] + b_i\right) \quad (3)$$

$$\tilde{C}^{(t)} = \tanh\left(w_c\left[h^{(t-1)}, x^{(t)}\right] + b_c\right) \quad (4)$$

where, w_i and b_i are the weight and intercept of input gate, w_c and b_c are the weight and intercept of cell state correction value.

Finally, the output is determined according to the current state information, the new cell state is obtained, and the hidden layer is updated. The expressions of the output gate, the current cell state and the hidden layer at the current moment are:

$$\Gamma_o = \sigma\left(w_o\left[h^{(t-1)}, x^{(t)}\right] + b_o\right) \quad (5)$$

$$C^{(t)} = \Gamma_i * \tilde{C}^{(t)} + \Gamma_f * C^{(t-1)} \quad (6)$$

$$h^{(t)} = \Gamma_o * \tanh C^{(t)} \quad (7)$$

where, w_o and b_o are the weight and intercept of the output gate, tanh is the hyperbolic tangent function.

As shown in Fig. 5, the BiLSTM model adopts a many-to-many output mode, each sequence contains 100 steps, and the output produces 100 classification results.

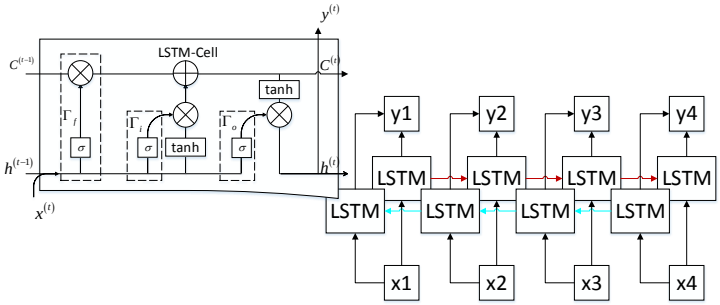

Figure 5. Structure of BiLSTM

The overall framework of the network is shown in Fig. 6, which consists of an input layer, two BiLSTM layers, two fully connected layers and an output layer. The input layer is input from the labeled feature set, and each feature sequence is a 100×3 data matrix, where 100 is the step size, corresponding to the index information of 100 peaks in the BCG sequence; 3 is the dimension, corresponding to the characteristic parameters of each peak, which are the peak amplitude and the distance between the peak and the adjacent two peaks. In order to play the role of expanding features, the labels are processed by one-hot encoding. The hidden layer has two BiLSTM layers and two fully connected layers. The first BiLSTM layer is set with 128 hidden layer units, and the second BiLSTM layer is set with 64 hidden layer units. The two fully connected layers are set with 32 and 16 hidden layer units respectively, and the activation function is set as a Rectified Linear Activation Function. The output layer uses the softmax activation function for logistic regression to classify the four output results. Adaptive moment estimation and cross-entropy loss function are used to optimize the network [18]. The network weights and biases are optimized after each iteration according to the value of the loss function.

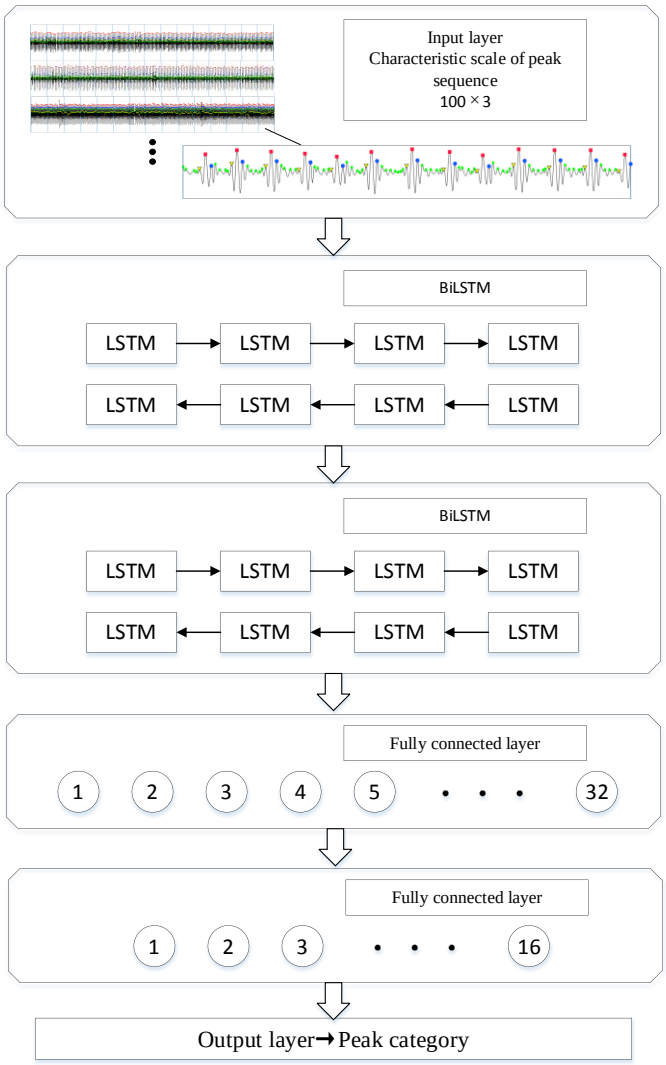

Figure 6. Heartbeat detection model framework based on BiLSTM

The data set contains 1190 feature sequences, which are divided in a ratio of 3:1. Data from 21 subjects was used as the training set and data from 7 subjects as the test set. The number of samples is 884 and 306 respectively, and the data is normalized before training. The main training parameters of the model are set as follows: the number of training epoch is 100, the sample batch size is 50, and the learning rate is 0.01. 20% of the training set data are set as the cross-validation set, and the two layers of BiLSTM are set with a dropout operation of 0.5 and 0.3 respectively to reduce overfitting.

3. Results

The evaluation method is as follows:

(1) Model evaluation. The classification performance of BiLSTM network was evaluated using accuracy (Acc), sensitivity (Se), specificity (Sp), precision (P), F1 score (F1) and confusion matrix.

(2) Heartbeat detection verification. The purpose of this paper is to locate the J peak, and the accuracy of J peak recognition is mainly verified by the number of heartbeats. The heartbeat detection results were evaluated using deviation rate (E), false positive rate (FPR), false negative rate (FNR), precision rate and recall rate.

(3) Statistical analysis. Based on the results of heartbeat detection, the statistical differences between BCG detection results and synchronized ECG were analyzed by paired sample t test and Pearson correlation coefficient.

3.1 Model Evaluation

When building the dataset, the setting of labels is essentially binary: J peak and non-J peak. Therefore, in the process of model evaluation, we only evaluate the recognition results of J wave. The test set data is predicted on the classification model, and the evaluation calculation results are: Acc =99.67%, Se =99.14%, Sp =99.78%, P =98.89%, $F1$ =99.01%. The confusion matrix of test set classification results is shown in Table I.

Table I. J peak classification confusion matrix of test set

Reference	Prediction	
	J peak	Non-J peak
J peak	5086	44
Non-J peak	57	25413

According to Table I and the evaluation calculation results, the model shows high accuracy in the classification of J peak and non-J peak. In order to verify the advantages of this model, we compared it with other popular sequence learning models. We established RNN, LSTM, and Gate Recurrent Unit (GRU) models for comparative experiments. The structure and parameter settings of the three models are consistent with the aforementioned BiLSTM model. Three experiments were performed for each model, and the results are shown in Table 2. It can be seen that the BiLSTM model has the highest average accuracy, which is 7.12%, 6.12%, and 3.67% higher than RNN, LSTM, and GRU.

Table II. Comparison of accuracy of different methods

Learning models	Accuracy			
	First time	Second time	Third time	Average
RNN	92.52%	91.33%	92.79%	92.21%
LSTM	93.97%	92.33%	93.32%	93.21%
GRU	95.99%	94.98%	96.02%	95.66%
BiLSTM	98.99%	99.67%	99.32%	99.33%

3.2 Heartbeat Detection Results

The J peak test results from one subject are selected for prior validation. The BCG signal is a mechanical signal of the heart that itself has non-strict periodicity, so the heartbeat location detected by the BCG signal lags behind the heartbeat location of the ECG, and the JJ interval varies slightly from the RR interval. Figure 7a shows the comparison between the BCG heartbeat detection results of the subject and the ECG, the square marks in the upper figure indicates the R peak location of the ECG, which

serves as the ground truth for this experiment. The square marks in the lower figure indicates the J peak labels of the BCG, and the vertical marks are the recognition results. It can be seen that the detection results correspond one-to-one with the ground truth. The results of JJ interval versus RR interval are shown in Figure 7b, which shows that the JJ interval and RR interval substantially coincide. Figure 7c is a Bland-Altman diagram of JJ interval versus RR interval, and it can be observed that detection results are basically in the 95% confidence zone, illustrating good agreement between JJ interval and RR interval detected herein within a certain margin of error.

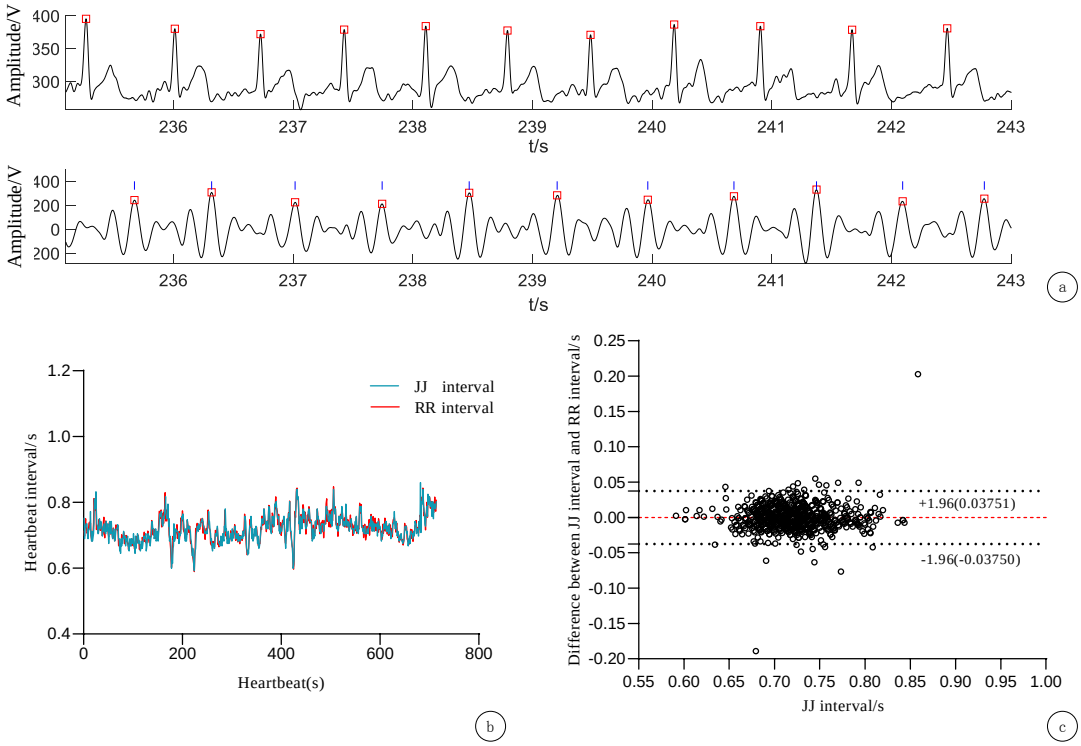

Figure 7. Comparison of calculation results between BCG and ECG: (a) Heartbeat detection, (b) Heartbeat interval, (c) Bland-Altman plot

Table III. Heartbeat detection results based on BiLSTM

Subject	Heartbeat(s)	TP	E%	FNR%	FPR%	Se%	P%
P22	674	672	0.30%	3.45%	0.82%	96.55%	96.28%
P23	680	680	0	0.73%	0.15%	99.27%	99.27%
P24	819	812	0.86%	1.69%	0.52%	98.31%	97.48%
P25	702	698	0.57%	0	0.08%	100%	99.57%
P26	714	714	0	0	0	100%	100%
P27	946	945	0.11%	0	0.02%	100%	99.89%
P28	609	609	0	0.16%	0.02%	99.84%	99.84%
Total	5144	5130	0.27%	0.85%	0.22%	99.15%	98.90%

Table III shows the detection results for subjects numbered P22 to P28 in the test set. The number of detected JJ interval is taken as the heartbeat detection result, TP is the number of heart rate labels in the test set, E is the deviation rate of the detection result, FNR is the false negative rate, FPR is the false positive rate, Se is the recall rate, and P is the precision rate. As can be seen from Table III, the average deviation rate of the subjects is only 0.27%, the accuracy of heartbeat detection is as high as 99.73%, and the average false negative rate does not exceed 1%. Only individual subjects had more false negative samples and the average false positive rate did not exceed 0.3%. In terms of recall rate and precision rate, the identification method herein reached 99.15% and 98.90%. In addition, we also use the same dataset to evaluate the performance of traditional threshold detection, template matching, and hierarchical clustering. Table IV shows the detection results of each method, the results show

that our method has a higher overall accuracy rate in the same field of study, can achieve high-precision heart rate monitoring requirements, and has a stronger expansion value.

Table IV. Comparison with other algorithms

Algorithms	E%	FNR%	FPR%	Se%	P%
Threshold detection	2.59%	6.04%	4.12%	94.15%	93.83%
Template matching	0.92%	2.68%	1.95%	97.41%	97.15%
Hierarchical clustering	1.86%	6.69%	0.72%	94.31%	94.08%
Proposed	0.27%	0.85%	0.22%	99.15%	98.90%

Table V. Comparison of statistical parameters of BCG and ECG signal characteristic parameters

Subject	HR_{ECG}/min^{-1}	HR_{BCG}/min^{-1}	*P*	*R*	RR interval /s	JJ interval /s	*P*	*R*
P22	71.11±2.75	71.33±2.73	0.894	0.945	0.841±0.031	0.840±0.032	0.889	0.923
P23	69.67±1.58	69.88±1.69	0.773	0.976	0.862±0.015	0.861±0.018	0.794	0.937
P24	80.63±3.14	81.18±3.12	0.738	0.916	0.722±0.043	0.718±0.052	0.721	0.835
P25	64.30±1.72	64.72±1.68	0.806	0.941	0.922±0.082	0.917±0.094	0.716	0.859
P26	67.18±0.83	67.22±0.86	0.908	0.985	0.884±0.068	0.885±0.068	0.954	0.966
P27	85.11±2.11	85.20±2.16	0.723	0.938	0.706±0.028	0.710±0.045	0.663	0.902
P28	68.38±1.88	68.81±1.35	0.827	0.948	0.880±0.036	0.877±0.051	0.814	0.821

3.3 Statistical Analysis

Based on the results of J peak detection, paired samples t test and Pearson correlation coefficient statistics were performed on the average heart rate and the successive heartbeat interval of the heartbeat detection results. The statistical results are shown in Table V. It can be seen from Table V that the heart rate and heartbeat interval calculated from BCG signals and ECG signals respectively have no significant difference (P>0.05). The Pearson correlation coefficients were all between 0.8 and 1.0, indicating that there was a strong correlation between the calculated results of the BCG signal and the ECG signal. The above statistical data show that within a certain error range, the heart rate calculated by the BCG signals can replace the reference heart rate of the ECG signals, which further illustrates the feasibility and accuracy of the heartbeat detection method herein.

4. Conclusion

This paper proposes a J peak detection method based on BCG peak sequence through the study of BCG peak sequence. This method does not rely on local time domain signals. By calculating the characteristic parameters of each wave peak in the BCG time series segment, and using the BiLSTM many-to-many recognition model, the method can directly classify the characteristic differences of BCG peak groups and efficiently detect the J peak in BCG. The data samples include BCG waveforms of different subjects in different sleeping positions, which are not limited to a single acquisition. In future work, based on the advantages of deep learning algorithms, the performance of this method can be further verified and improved under the condition of expanding the training set. In addition, in order to achieve heart rate monitoring in groups with heart-related diseases, we need to continue to study the feature extraction methods.

References

[1] E. J. Benjamin et al. “Heart disease and stroke statistics-2019 update a report from the american heart association,” Circulation, vol. 139, no. 10, pp. e56–e528, Mar. 2019.

[2] He S, Dajani H R, Meade R D, et al. “Continuous Tracking of Changes in Systolic Blood Pressure using BCG and ECG,” Annu Int Conf IEEE Eng Med Biol Soc, vol. 2019, pp. 6826-6829 Jul. 2019.

[3] González-Landaeta R, Casas O, Pallàs-Areny R. “Heart rate detection from an electronic weighing scale,” Physiological measurement, vol. 29, no.8, pp. 979-988, Jul. 2008.

[4] Da H D, Winokur E S, Sodini C G. “A continuous, wearable, and wireless heart monitor using head ballistocardiogram (BCG) and head electrocardiogram (ECG),” Annu Int Conf IEEE Eng Med Biol Soc, vol. 2011, pp. 4729-4732, 2011.

[5] Inan O T, Migeotte P F, Park K S, et al. “Ballistocardiography and seismocardiography: A review of recent advances,” IEEE Journal of Biomedical and Health Informatics, vol.19, no. 4, pp. 1414-1427, Jul. 2015.

[6] Shin J H, Hwang S H, Chang M H, Park K S. “Heart rate variability analysis using a ballistocardiogram during Valsalva manoeuvre and post exercise.” Physiological Measurement, vol.32, no. 8, pp. 1239-1264, Jul. 2011.

[7] Choi B H, Chung G S, Lee J S, Jeong D U, Park K S. "Slow-wave sleep estimation on a load-cell-installed bed: a non-constrained method," Physiol Meas, vol. 30, no. 11, pp. 1163-1170, Oct. 2009.
[8] D. Heise and M. Skubic. "Monitoring pulse and respiration with a non-invasive hydraulic bed sensor," Annu Int Conf IEEE Eng Med Biol Soc, vol. 2010, pp. 2119–2123, 2010.
[9] Shin J H, Choi B H, Lim Y G, Jeong D U, Park K S. "Automatic ballistocardiogram (BCG) beat detection using a template matching approach," Annu Int Conf IEEE Eng Med Biol Soc, vol. 2008, pp. 1144-1146, 2008.
[10] Q Xie et al. "A personalized beat-to-beat heart rate detection system from ballistocardiogram for smart home applications," IEEE Trans Biomed Circuits Syst, vol. 13, no. 6, pp. 1593–1602, Dec. 2019.
[11] Brüser C, Stadlthanner K, Brauers A, Leonhardt S. "Applying machine learning to detect individual heart beats in ballistocardiograms," Annu Int Conf IEEE Eng Med Biol Soc, vol. 2010, pp. 1926-1929, 2010.
[12] Shen G, Yang M Q, Zhang B Y. "Ballistocardiogram-Based Heart Rate Variation Monitoring Using Unsupervised Learning," Advances in Transdisciplinary Engineering, 2018, 7.
[13] Murat F, Yildirim O, Talo M, Baloglu U B, Demir Y, Acharya U R. "Application of deep learning techniques for heartbeats detection using ECG signals-analysis and review," Computers in Biology and Medicine, vol. 120, pp. 103726, Mar. 2020.
[14] Faust O, Shenfield A, Kareem M, San T R, Fujita H, Acharya U R. "Automated detection of atrial fibrillation using long short-term memory network with RR interval signals," Computers in Biology and Medicine, vol. 102, no. 2018, pp. 327-335, Nov. 2018.
[15] Yildirim Ö. "A novel wavelet sequence based on deep bidirectional LSTM network model for ECG signal classification," Computers in Biology and Medicine, vol. 96, no. 2018, pp. 189-202, May. 2018.
[16] Jiao C, Chen C, Gou S, et al. "Non-Invasive Heart Rate Estimation From Ballistocardiograms Using Bidirectional LSTM Regression," IEEE J Biomed Health Inform, vol. 25, no. 9, pp. 3396-3407, Sep.2021.
[17] Malešević N, Petrović V, Belić M, Antfolk C, Mihajlović V, Janković M. "Contactless Real-Time Heartbeat Detection via 24 GHz Continuous-Wave Doppler Radar Using Artificial Neural Networks," Sensors (Basel), Vol. 20, no. 8, pp. 2351, Apr. 2020.
[18] Wael Ahmad A1Zoubi. "A Survey of Clustering Algorithms in Association Rules Mining," International Journal of Computer Science and Information Technology, vol.11, no. 2, 2019.
[19] Wu S, et al. "Deep learning in clinical natural language processing: a methodical review," Journal of the American Medical Informatics Association, vol. 27, no. 3, pp. 457-470, Mar. 2020.